

Antidepressants escitalopram and venlafaxine up-regulate *BDNF* promoter IV but down-regulate neurite outgrowth in differentiating SH-SY5Y neurons

Denis Zosen^a, Elena Kondratskaya^{b,c}, Oyikum Kaplan-Arabaci^a, Fred Haugen^d, Ragnhild Elisabeth Paulsen^{a,*}

^a Section for Pharmacology and Pharmaceutical Biosciences, Department of Pharmacy, Faculty of Mathematics and Natural Sciences, University of Oslo, Oslo, Norway

^b Department of Medical Genetics, Oslo University Hospital, Oslo, Norway

^c NORMENT, Institute of Clinical Medicine, University of Oslo, and Division of Mental Health and Addiction, Oslo University Hospital, Oslo, Norway

^d Department of Work Psychology and Physiology, National Institute of Occupational Health (STAMI), Oslo, Norway

ARTICLE INFO

Keywords:

Antidepressants
BDNF
Escitalopram
Neuronal differentiation
SH-SY5Y
Venlafaxine

ABSTRACT

Antidepressants are used to treat depression and some anxiety disorders, including use in pregnant patients. The pharmacological actions of these drugs generally determine the uptake and metabolism of a series of neurotransmitters, such as serotonin, norepinephrine, or dopamine, along with an increase in BDNF expression. However, many aspects of antidepressant action remain unknown, particularly whether antidepressants interfere with normal neurodevelopment when taken by pregnant women. In order to reveal cellular and molecular implications crucial to the functioning of pathways related to antidepressant effects, we performed an investigation on neuronally differentiating human SH-SY5Y cells. To our knowledge, this is the first time human SH-SY5Y cells in cultures of purely neuronal cells induced by controlled differentiation with retinoic acid are followed by short-term 48-h exposure to 0.1–10 μ M escitalopram or venlafaxine. Treatment with antidepressants (1 μ M) did not affect the electrophysiological properties of SH-SY5Y cells. However, the percentage of mature neurons exhibiting voltage-gated sodium currents was substantially higher in cultures pre-treated with either antidepressant. After exposure to escitalopram or venlafaxine, we observed a concentration-dependent increase in activity-dependent *BDNF* promoter IV activation. The assessment of neurite metrics showed significant down-regulation of neurite outgrowth upon exposure to venlafaxine. Identified changes may represent links to molecular processes of importance to depression and be involved in neurodevelopmental alterations observed in postpartum children exposed to antidepressants antenatally.

1. Introduction

Antidepressant drugs (ADDs) have been used to treat depression during pregnancy with controversial results (Olivier et al., 2015; Nulman et al., 1997; Szegda et al., 2014; Dubovicky et al., 2017); both treated and untreated depression led to different neurodevelopmental alterations in the offspring. Nowadays, SSRI (selective serotonin reuptake inhibitor, e.g., escitalopram) but also SNRI (serotonin and norepinephrine reuptake inhibitor, e.g., venlafaxine) are the pharmacological choice for ADD treatment during pregnancy (Alwan et al., 2011; Vigod et al., 2016). Those ADDs are typically regarded as non-teratogenic and safe to use during pregnancy. Nevertheless, antenatal use of ADDs has been linked to neurological and behavioral problems in children (Olivier

et al., 2015; Brandlistuen et al., 2015), with a small increased risk of congenital malformations (Olivier et al., 2015; Chambers et al., 1996; Udechuku et al., 2010). Neurodevelopmental deviations, such as autism spectrum disorders (ASD) (Rai et al., 2013; Fatima et al., 2018), attention-deficit/hyperactivity disorder (ADHD) (Lessem et al., 2021), anxiety (Brandlistuen et al., 2015), and abnormal psychomotor development (Mortensen et al., 2003), were observed in postpartum children exposed to ADDs prenatally. The World Health Organization does not recommend ADDs use during pregnancy due to restrictions associated with human subjects research and, thus, lack of medical studies determining the teratogenic risk level (Kautzky et al., 2022). Recently the importance and need for molecular and mechanistic analyses associated with ADDs treatment during pregnancy were highlighted (Gentile and Fusco, 2017; Thompson et al., 2009).

* Corresponding author. Section for Pharmacology and Pharmaceutical Biosciences, Department of Pharmacy, University of Oslo, PO Box 1068 Blindern, N-0316, Oslo, Norway.

E-mail address: r.e.h.paulsen@farmasi.uio.no (R.E. Paulsen).

<https://doi.org/10.1016/j.neuint.2023.105571>

Received 24 January 2023; Received in revised form 26 June 2023; Accepted 4 July 2023

Available online 13 July 2023

0197-0186/© 2023 The Authors. Published by Elsevier Ltd. This is an open access article under the CC BY license (<http://creativecommons.org/licenses/by/4.0/>).

Abbreviations

ADDs	antidepressant drugs
DIV	differentiation day <i>in vitro</i>
RA	retinoic acid
TUBB3	tubulin β class III

Even though many studies have shown the effectiveness of ADDs in treating depression, their mechanism of action is not yet fully understood. The classical theory of the effects of ADDs is the monoamine hypothesis, particularly the role of 5-hydroxytryptamine (5-HT; serotonin) (Schildkraut, 1965; Coppen, 1967; Albert et al., 2012). Thus, the majority of pharmacological treatments are concentrated around this target. In addition, ADDs increase brain-derived neurotrophic factor (BDNF) activity in the brain, and this has been proposed as an essential part of the ADDs mechanism of action (Lee and Kim, 2010; Castrén and Monteggia, 2021). New studies show that ADDs can act directly through the BDNF receptor, tropomyosin-related kinase receptor type B (TrkB) (Casarotto et al., 2021). 5-HT and BDNF have different roles in developing versus adult brains (Herenius and Lagercrantz, 2001; Agholme et al., 2010). Therefore, we hypothesized that ADDs, through direct or indirect effects on 5-HT- and/or BDNF levels, can interfere with normal neuronal development.

Among the indicators of neurodevelopment as well as neuroregeneration *in vitro*, neurite outgrowth stands out as the most critical determinant of neuronal cell morphology and connectivity. Only a couple of studies focusing on the effects of ADDs on neurite outgrowth in neuronal cell lines have been published, in rat pheochromocytoma cells (PC12) (Meng et al., 2019; Gao et al., 2020). Considering this unknown territory in the field, more studies are required on different cell lines for a better understanding of ADDs.

Human SH-SY5Y cells have been extensively used in neuropharmacological and neurotoxicological studies. Additionally, these cells can be differentiated into different neuronal lineages, including monoaminergic neurons, and are responsive to different neurotrophic factors (Agholme et al., 2010; Kovalevich and Langford, 2013). Thus, SH-SY5Y can serve as a solid cellular model to assess neurodevelopmental alterations under exposure to ADDs. Herein, we approached SH-SY5Y cells with a simple and reproducible neuronal differentiation protocol by RA-induced differentiation for 21-day *in vitro*. We also assessed the effects of ADDs on neuron electrophysiology features, BDNF promoter activity, and neurite outgrowth at different concentrations on the last two days of differentiation.

2. Materials and methods

2.1. Pharmaceuticals and reagents

Escitalopram oxalate (Tocris, 4796), venlafaxine hydrochloride (Tocris, 2917), both at 50 mM stock concentrations, and serotonin (5-hydroxytryptamine, 5-HT) hydrochloride (Sigma, H9523), and L-norepinephrine hydrochloride (Sigma, 74480) both at 10 mM stock, were dissolved in sterile ddH₂O and stored at -20°C and used freshly avoiding freezing-thawing cycles. Recombinant BDNF (450-02) was from Peprotech, anti-BDNF antibodies (AB1513P) from Millipore, and TrkA receptor inhibitor GW 441756 (2238) was purchased from Tocris.

2.2. Neuronal differentiation of SH-SY5Y cells

Human neuroblastoma SH-SY5Y cells (ATCC, CRL-2266), at passage numbers between 9 and 15, were split at least twice after thawing and prior to initiating the differentiation protocol. The cells were grown on 100-mm dishes in a culture medium based on DMEM with L-glutamine

(ThermoFisher, 42430025) supplemented with 10% FBS (Lonza, DE14-801F), 1% pyruvate (ThermoFischer, 1360-070), and 1% penicillin-streptomycin (ThermoFischer, 15140-122). Once the cells reached a confluence of $\sim 70\text{--}80\%$, neuronal differentiation was induced in the culture medium based on DMEM with L-glutamine supplemented with 1% FBS, 1% pyruvate, 1% penicillin/streptomycin, and 10 μM all-trans retinoic acid ("RA", from a 20 mM stock in DMSO; BioGems, 3027949). The culture medium was refreshed every Monday, Wednesday, and Friday, lasting 21 days, termed differentiation day *in vitro* (DIV) -0 to -21 (Fig. 1). At approx. DIV14 cells changed their morphology to more neuron-like, with distinguishable neurites and clusterization. On DIV17, cells were harvested with Accutase (ThermoFisher, A1110501) for 5 min at $+37^{\circ}\text{C}$ and spun down at 900 rpm for 5 min. One 100-mm dish resulted in approx. $5\text{--}15 \times 10^6$ cells total yield. The cells were re-plated on 6-, 24-, or 96-well plates. All plates were pre-coated with 5 $\mu\text{g}/\text{cm}^2$ of poly-L-lysine hydrobromide ("PLL"; Sigma, P2636) in ddH₂O for 1 h at room temperature (RT), which was followed by removal of PLL and air-drying; and then with 5 $\mu\text{g}/\text{cm}^2$ of Cultrex Basement Membrane Matrix ("ECM"; Bio-Techne, 3434-010-02) in ice-cold DMEM for 1 h at $+37^{\circ}\text{C}$, which was discarded immediately prior to seeding of the cells. The culture consisted of $>99\%$ live neurons, confirmed by labeling with NeuroFluor NeuO (STEMCELL Technologies, 01801) membrane-permeable fluorescent probe, 20 nM for 1 h at $+37^{\circ}\text{C}$. The exposure to pharmaceuticals was initiated on DIV19, for 48 h, in the differentiation culture medium, and the effects of ADDs were assessed on DIV21 (Fig. 1).

2.3. Immunofluorescent staining

For immunostaining, differentiating SH-SY5Y cells were seeded onto lumox 96-well black plates with a transparent bottom (Sarstedt, 94.6120.096) at the concentration of 1.5×10^4 cells/well in the differentiation culture medium. The cells were washed once with 1xPBS, fixed in ice-cold 99% methanol for 10 min, and stored at -20°C until immunostaining. Next, the fixed cells were washed thrice with cold 1xPBS. The cells were incubated in blocking buffer (1xPBS containing 0.05% Tween 20, 2.5% BSA, and 1% normal goat serum) for 1 h at room temperature (RT) or overnight at $+4^{\circ}\text{C}$. Then, the blocking buffer was discarded and substituted with a blocking solution containing primary antibodies (rabbit anti-TUBB3 (tubulin β class III; 1:2000, Sigma, T2200) and mouse anti-GFAP (glial fibrillary acidic protein; 1:1000, Cell Signaling Technology, 3670)) overnight at $+4^{\circ}\text{C}$. The following day, cells were washed thrice with cold 1xPBS and incubated with secondary antibody (goat anti-rabbit Alexa Fluor Plus 488 (ThermoFisher, A32731) and goat anti-mouse Alexa Fluor Plus 594 (ThermoFisher, A32742), both at 1:1000 dilution) for 1 h at RT. Next, the cells were washed thrice with 1xPBS, and the samples were maintained in 1xPBS at $+4^{\circ}\text{C}$ until imaging. Immunofluorescence was imaged at $10\times$ magnification using the InCuCyte ZOOM (Essen BioScience) live-cell imaging platform, with exposure times of 550 ms (green channel) and 950 ms (red channel). Immunostaining for MAP2 (microtubule-associated protein 2; 1:5000; Abcam, Ab5392), SYP (synaptophysin; 1:200; Abcam, Ab14692), and PSD-95 (postsynaptic density protein 95; 1:300; Abcam, Ab13552) with DAPI (4',6-diamidino-2-phenylindole; 1:1000; ThermoFisher, 62248), was performed as previously described (Lauvås et al., 2022). Immunofluorescence was assessed with the CellInsight CX7 High Content Analysis Platform (ThermoFisher).

2.4. Western blotting

Proteins from SH-SY5Y cells seeded in 6-well plates washed with 1x PBS were isolated by using RIPA buffer containing three protease inhibitors (leupeptin 5 $\mu\text{g}/\mu\text{L}$, pepstatin A 1 $\mu\text{g}/\mu\text{L}$, phenylmethylsulfonyl fluoride 300 μM) and the phosphatase inhibitor Na_3VO_4 (300 μM). After measuring the protein concentration with the BCA Protein Assay Kit (Pierce, 23225), samples were harvested in Laemmli buffer

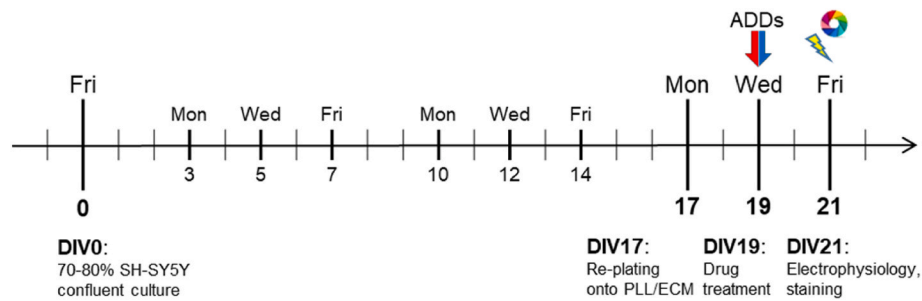


Fig. 1. SH-SY5Y differentiation protocol design and experimental timeline. Abbreviations: ADDs, antidepressant drugs; DIV, differentiation day *in vitro*; ECM, extracellular matrix; PLL, poly-L-lysine.

supplemented with 5% mercaptoethanol and denatured by incubating at 95 °C for 5 min. Protein samples (20 µg) were loaded and run on SDS-PAGE gels (Bio-Rad, 4551095), using the Bio-Rad Mini-PROTEAN® electrophoresis system. The blots were analyzed with the primary antibodies SYP, PSD-95, MAP2 and TUBB3 as explained above. β -ACTIN (1: 5000; Sigma; A5346) antibody was used as loading control, and membranes were further incubated with Odyssey secondary antibodies goat anti rabbit (GAR) 800 and 680, and goat anti mouse (GAM) 680 (1: 10000; LICOR). Odyssey® CLx Infrared Imaging System was used for quantitative analysis for detected bands. The signal intensity ratios of the proteins of interest were normalized to internal standard (β -ACTIN) and presented as relative to the average of controls.

2.5. Electrophysiological studies in SH-SY5Y-derived neurons

For electrophysiological experiments, differentiating SH-SY5Y neurons were seeded at DIV17 onto 24-well plates (Nunc, 143982) with 12 mm round glass coverslips coated with PLL/ECM at a concentration of 2×10^5 cells/well. On DIV21, the coverslips were transferred to a submersion chamber perfused with artificial cerebrospinal fluid ("aCSF"; containing in mM: 150 NaCl, 5 KCl, 1 MgSO₄, 2 CaCl₂, 10 glucose, 10 HEPES; pH 7.4; 300–310 mOsm/L). Tetrodotoxin citrate (TTX, 1 µM; Alomone Labs, T-550) was used to confirm TTX-sensitivity. The same procedure was used for SH-SY5Y undifferentiated cells. The neurons were visually identified with an up-right infrared-differential interference contrast (IR-DIC) microscope (Olympus BX51WI) and captured with a CoolSNAP EZ with SSD ICX285 (Photometrics) video camera. Patch electrodes were fabricated from borosilicate glass capillaries using a vertical puller (PC-10; Narishige). The pipette solution contained (in mM): 100 CsF, 40 CsCl, 5 NaCl, 0.5 CaCl₂, 10 HEPES, 2 EGTA, 2 Mg-ATP. Pipette solution aliquots were freshly made and filtered, osmolarity was 290 mOsm/L, and patch pipette resistance was 8–10 MOhm. All recordings were performed using a Multi-Clamp 700B amplifier (Molecular Devices). Recordings and pre-processing of data were made with WinWCP (University of Strathclyde). The signals were typically low-pass filtered with a corner frequency ($\times 0.005.3$ dB) of 3 kHz and sampled at 6 kHz by DigiData 1322A (Molecular Devices). Recordings were performed in a voltage clamp (recording of Na⁺/K⁺ currents) or current-clamp mode (action potential activation due to step current injection), applying the standard protocols. V_h = –60mV, unless otherwise stated. Data analysis was performed with p-CLAMP 10 (Molecular Devices) and OriginLab 8 (OriginLab Corp.).

2.6. Cytosolic calcium detection

The cells from 2.5. were tested for spontaneous calcium transients as a functional assessment in Ca²⁺-imaging experiments. The SH-SY5Y neurons were loaded with 1 µM Cal-520 (Cal-520 a.m.; Abcam, ab171868) calcium dye-containing aCSF for 30 min at +37 °C and then transferred to the recording chamber containing standard aCSF. The images were recorded with an upright microscope (Axioskop FS, Carl

Zeiss) using a Zeiss W Plan-Apochromat 421462-99-00 40x/1.0 DIC VIS-IR $\infty/0$ objective, combined with the Andor iXon Ultra 897 camera. Image representation of time series was acquired at 10 Hz (512 × 512 pixels) for 5 min. WinFluor software was used to analyze live calcium traces and derive various parameters reflecting the characteristics of cellular calcium signals. Fluorescence traces were normalized to the initial fluorescence intensity ($\Delta F/F_0$).

Differentiating SH-SY5Y neurons were plated onto black 96-well plates (Corning, 3340, or 3603) with a transparent glass bottom at 2×10^4 cells/well concentration. On DIV21, SH-SY5Y neurons were exposed to 4 µM Fura-2/acetoxymethyl ester (Fura-2/AM; Santa Cruz, 108964-32-5) in a 100 µL/well culture medium for 30 min at +37 °C and 5% CO₂. All following wash steps and drug exposures were performed in Normal buffer (containing in mM: 140 NaCl, 3.5 KCl, 15 Tris-HCl pH 7, 1.2 Na₂HPO₄ × NaH₂PO₄ pH 7.4, 5 glucose, 2 CaCl₂, in ddH₂O). After pre-treatment with Fura-2/AM, it was de-esterified by incubation with 1 mM MgSO₄ in Normal buffer for 10 min and washed twice before the baseline was measured. Subsequently, the wash buffer was replaced with test compounds in Normal buffer, and the [Ca²⁺]_i value was measured 120-min post-treatment. The [Ca²⁺]_i was measured by detecting Fura-2 fluorescence using CLARIOstar microplate reader (BMG Labtech), simultaneously assessing ratiometric F₃₄₀/F₃₈₀ [Ca²⁺]_i (Ex: 340 [Ca²⁺-bound]/380 [Ca²⁺-unbound] nm, Em: 510 nm). N-Methyl-D-aspartic acid (NMDA; Sigma, M3262) and glycine (Sigma, G8790), as well as a selective non-competitive NMDA receptor antagonist (+)-MK-801 hydrogen maleate (Sigma, M107), were used in control experiments. The average background autofluorescence from wells containing cells without Fura-2/AM was subtracted from excitations at 340 nm, and 380 nm before the 340/380 ratio was calculated.

2.7. Plasmid transfection and luciferase assay

Differentiating SH-SY5Y neurons on DIV17 were plated on 6-well plates (Eppendorf, 0030720113) at 7×10^5 cells/well. The K2 Transfection System (Biont, T060–0.75) was used according to the recommendations of the manufacturer. On DIV18, cells were transfected with pGL4.15 *BDNF* pIV (–204/+320) *Firefly* luciferase plasmid (0.8 µg; a kind gift from Prof. Tönis Timmusk (Pruunsild et al., 2011)) and internal control vector pRL-CMV *Renilla* luciferase plasmid (0.2 µg; Promega, E2261) to a total of 1 µg DNA/mL culture medium overnight at +37 °C and 5% CO₂. Then, the cells were exposed to escitalopram or venlafaxine at different concentrations in a fresh differentiation culture medium on DIV19. After 48 h, on DIV21, *Firefly* luciferase was measured by detecting the reaction with D-luciferin (ThermoFisher, 88291), and *Renilla* luciferase was measured using the Dual-Luciferase Reporter Assay System (Promega, E1910) kit, in a luminometer (EG&G Berthold Lumat LB9507) as previously described (Strøm et al., 2010). The *Firefly*/*Renilla* bioluminescence ratios were calculated, and the results are presented as normalized values relative to the average of controls.

2.8. Live-cell imaging and neurite outgrowth

Differentiating SH-SY5Y neurons were seeded at a concentration of 1.5×10^4 cells/well for neurite metrics onto TPP 96-well plates (TPP Techno Plastic Products AG, 92096) in a 150 μ L/well volume of differentiation culture medium to observe neurite regrowth or the impact on regrowing potency of cells after cell reseeded. The IncuCyte ZOOM live-cell analysis system (Essen BioScience) was used to assess cellular metrics with an automated NeuroTrack software module (Essen

BioScience, 9600-0010) module. Plates were scanned every 4 h over a 48-h period using a 10 \times objective. Four images per well were captured, and images were analyzed for neurite length. The masks/filters adjustments for the Neurotrack phase-contrast image analysis were as follows: Segmentation mode: Texture; Hole fill: 0; Adjust size: -5μ m; Min cell width: 8 μ m; Neurite filtering: Best; Neurite sensitivity: 0.35 μ m; and Neurite width: 1 μ m. The following parameter was quantified: Neurite Length = sum of lengths of all neurites pooled/area of the image field.

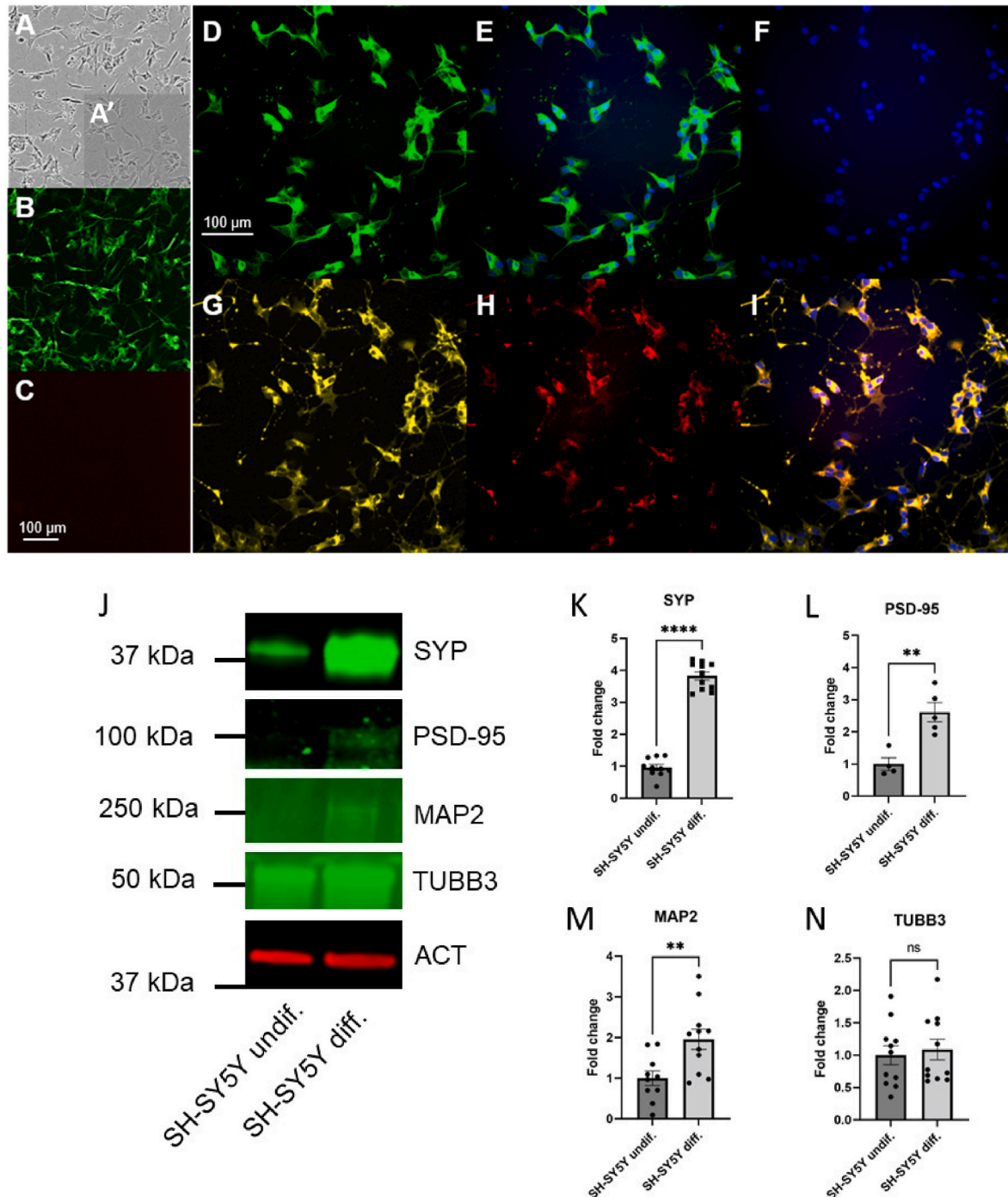


Fig. 2. Differentiating SH-SY5Y cells on DIV21: Phase-contrast (A) and immunofluorescence staining for TUBB3 (B) neuronal and GFAP (C) glial markers on DIV21. (A') shows undifferentiated SH-SY5Y cells. High content imaging, D: MAP2, E: merge MAP2 and DAPI, F: DAPI, G: SYP, H: PSD-95, I: merge SYP and PSD-95 with DAPI. J: Comparison of synaptic protein levels between differentiated and undifferentiated SH-SY5Y cells by quantitating Western Blotting. Quantifications for presynaptic marker SYP (K), postsynaptic marker PSD-95 (L), marker for mature neuron MAP2 (M), marker for immature neuron TUBB3 (N). Data were normalized to β -actin and analyzed with Student's *t*-test. ***p* < 0.01, ****p* < 0.001 *****p* < 0.0001, ns: non-significant.

2.9. Statistical analysis

Data are presented as mean \pm standard deviation (SD), for live-cell imaging with InCuCyte, results are presented as mean \pm standard error of the mean (SEM), with replicates $n \geq 3$ –6 per group. Mann-Whitney *U* test, Student's *t*-test, one-way or two-way analysis of variance (ANOVA), with Dunnett's or Tukey's multiple comparisons test (MCT), respectively, were used as described in each figure legend to determine a significant difference between treatments and controls at $\alpha = 0.05$. A *p*-value of <0.05 was considered significant (* $p < 0.05$, ** $p < 0.01$, *** $p < 0.001$, **** $p < 0.0001$). For the InCuCyte data, all time points and repeated measures data were used to build and run the analysis. All data were analyzed using GraphPad Software 8.2.

3. Results

3.1. Characterization of differentiating SH-SY5Y cultures

Three weeks (differentiation day *in vitro* 21, DIV21) after neuronal differentiation induction with 10 μ M RA (see Fig. 1 for experimental design; Fig. 2 A, phase contrast, A' undifferentiated), 100% of SH-SY5Y cells were live neurons (positive labeling for NeuO, not shown), as well as expressing neuron-specific class III beta-tubulin (Fig. 2 B: TUBB3). No cells were found to be GFAP-positive (Fig. 2 C). Additionally, high-content imaging for MAP2, SYP, and PSD-95 proved the culture to be neuron-specific, expressing all three neuronal markers (Fig. 2, D-I; Suppl. Fig. 1). Most of the cells co-expressed both SYP and PSD95, indicating the formation of synaptic machinery. Western blotting data clearly showed a significant difference between undifferentiated and differentiated SH-SY5Y cells in terms of presynaptic marker SYP, post-synaptic marker PSD-95, and mature neuron marker MAP2 (Fig. 2J–N), whereas the marker of more immature neurons TUBB3 did not change. Suppl. Fig. 1 shows MAP2 immunofluorescence from undifferentiated and differentiated cells, highlighting their difference in morphology.

To prove that differentiated SH-SY5Y cells are mainly neuronal in

nature by electrophysiological means, we compared their properties with undifferentiated cells at the same time point (21 DIV, negative control) and mouse cortical neurons were used as a positive control (mouse 14–16 PND, Suppl. Fig. 2). Individual cells were visually selected (Fig. 3 A, C) for recordings based on their morphology and assayed for physiological properties.

In the voltage step protocol (from -80 mV to $+40$ mV with 10 mV step), inward and outward currents were recorded in some portion of cells. The representative original traces of recorded transmembrane currents and corresponding current-voltage relation curve for inward sodium currents are shown in Fig. 3 B, D. Inward currents were reversibly inhibited by tetrodotoxin (TTX) 1 μ M (data not shown), justifying that those inward currents are mediated by TTX-sensitive sodium channels. In a current clamp-mode with step current injection, none of the recorded cells showed action potential activation regardless of group (data not shown).

Since SH-SY5Y cells endogenously express several Nav isoforms including Na v 1.2 and Na v1.7 (Vetter et al., 2012), with standard voltage step protocol we recorded inward Na⁺ currents in whole cell voltage clamp mode from 6 out of 10 cells. The comparison of averaged normalized IV curves for all cells shows that in undifferentiated cells the sodium IV curve is largely shifted to high depolarizing potentials with current maximum activated around 0 mV that corresponds to those previously reported by Toselli (Toselli et al., 1996). The maximum current activation potential for differentiated cells was estimated around -40 – -35 mV and curve shape is common for non-mature rodent neurons (comparison with mouse cortical neurons shown in Suppl. Fig. 2).

We also compared the maximum sodium currents amplitude range for differentiated versus undifferentiated cells. As shown in Fig. 3F, in undifferentiated cells sodium current amplitudes were significantly smaller (** $p < 0.01$, Mann-Whitney *U* test) than ones recorded from differentiated cells, most probably because of small cell size and low channel density. These data are in agreement with previously reported properties of Na channels expressed in undifferentiated SH-SY5Y cells

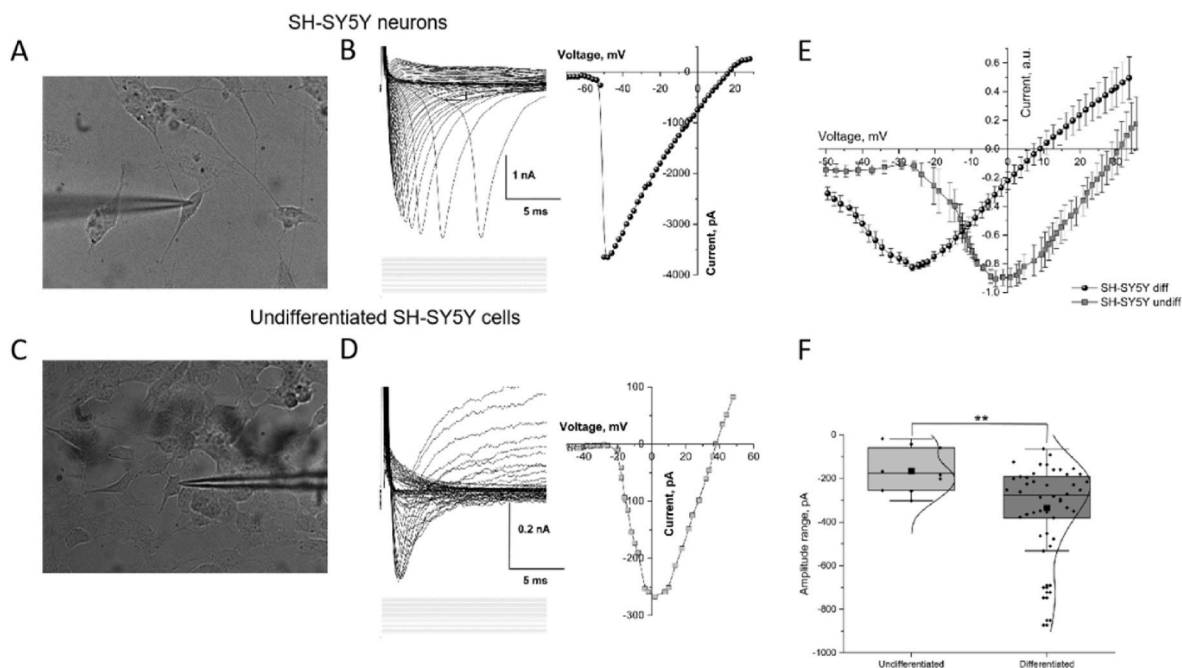


Fig. 3. Differentiated SH-SY5Y neurons on DIV21 in the electrophysiological template: A, C: SH-SY5Y neuron and undifferentiated SH-SY5Y cell used in the patch-clamp experiment, differential interference contrast (DIC) microscopy image. B, D: Voltage-clamp recording of whole cell currents in the neuron representing the activation of Na⁺ and K⁺ currents and in undifferentiated SH-SY5Y cell. Each trace represents recordings from a single voltage step in the neuron as shown in stimuli protocol below the trace. E: Averaged normalized current-voltage (IV) curves for sodium currents recorded in SH-SY5Y neurons versus SH-SY5Y undifferentiated cells. F: The range of sodium current maximum amplitudes in differentiated SH-SY5Y neurons and undifferentiated cells. (** $p < 0.01$, Mann-Whitney *U* test).

versus RA differentiated, and show about 2-fold increase in the sodium currents amplitude upon differentiation (Toselli et al., 1996).

The waveform of current-voltage relation for K^+ currents was also substantially different for differentiated versus undifferentiated cells. The functional changes in potassium conductance of SH-SY5Y upon differentiation was previously described (Tosetti et al., 1998), but was not examined in this study (Suppl. Fig. 2).

SH-SY5Y neurons labeled with Cal-520 showed spontaneous Ca^{2+} transients (Fig. 4A and B). To assess whether differentiating SH-SY5Y neurons can be used to determine cytosolic calcium changes, we used cultures on DIV21 and Fura-2 calcium-sensitive fluorescent probe to examine Ca^{2+} -influx under exposure to NMDA receptor antagonist (MK-801) or NMDA receptor agonist (NMDA/glycine). After 120-min exposure, we observed a 53% reduction in cytosolic calcium influx with non-competitive NMDA receptor antagonist MK-801 and a 28% increase under exposure to NMDA/glycine ($P < 0.0001$, Fig. 4, C).

3.2. Electrophysiological assessment revealed more cells exhibiting activation of Na^+ currents in SH-SY5Y neurons pre-exposed to antidepressants

For electrophysiological assessment, we chose a single concentration of ADDs (1 μ M) for treatment for both drugs. In total, 89 cells were recorded in all electrophysiology experiments (30 cells in control, 34 – in escitalopram, and 25 – in venlafaxine groups). Voltage-gated sodium currents were recorded from neurons in each group: control ($n = 6$, i.e., 20%), escitalopram ($n = 10$, i.e., 29%), and venlafaxine ($n = 13$, i.e., 52%).

The neurons were kept at a holding potential of -80 mV, and Na^+ currents were recorded within a range of -60 mV to -80 mV before the stimulation protocol for each cell. Under these conditions, Na^+ currents exhibited a typical voltage-dependent activation with a threshold of activation between -60 and -50 mV and a maximum peak current of about -20 mV (Fig. 5, A-C) in cells from all groups. Corresponding current-voltage curves (I/V curves) for the peak Na^+ currents were normalized to the maximum current amplitude. No significant difference in threshold voltage for maximum conductance was found, indicating no changes in the intrinsic properties of cells between groups of tested drug exposure.

3.3. Cytosolic calcium was not affected by treatment with antidepressants in differentiating SH-SY5Y neurons

We further studied the underlying mechanisms of escitalopram and venlafaxine actions in differentiating neurons. Previously, reports indicated an increased calcium influx in astrocytes treated with ADDs

sertraline and paroxetine (Then et al., 2017). Thus, we used Fura-2 as a calcium-sensitive probe to assess the effects of ADDs on cytosolic calcium in SH-SY5Y neurons. Exposure to either escitalopram or venlafaxine did not have any significant effect on calcium influx 120 min post-treatment, though a slight positive trend could be observed for both escitalopram and venlafaxine (Fig. 6). Likewise, neither norepinephrine (NE) nor serotonin (5-HT) had any effect on cytosolic calcium influx.

3.4. Antidepressants up-regulated activity-dependent BDNF promoter IV in differentiating SH-SY5Y neurons

Since it is known that ADDs can act through BDNF (Castrén and Monteggia, 2021), which in turn is affected by Ca^{2+} signaling (He et al., 2005; Tao et al., 2002), we analyzed the effect of escitalopram and venlafaxine on activity-dependent human BDNF promoter IV (Pruunsild et al., 2011). Both ADDs concentration-dependently up-regulated the BDNF promoter IV in differentiating SH-SY5Y neurons (Fig. 7), supporting the increased number of cells with sodium currents (3.2., first paragraph).

3.5. TUBB3 was not significantly changed in differentiating SH-SY5Y neurons under exposure to antidepressants

The neuron-specific class III beta-tubulin, also known as TUBB3 or Tuj1, is expressed in the post-mitotic neuron cytoskeleton (Katsetos et al., 2003) and thus may be used as an early maturation marker for neurons. Differentiating SH-SY5Y neurons were immunostained for TUBB3 on DIV21, 48 h post-exposure to drugs. After exposure to either ADD, no visible morphological differences between groups were observed for TUBB3 staining. Quantification of TUBB3-labeled fluorescence intensities in the microplate reader showed a slight trend to higher immunofluorescence intensity (Fig. 8) for escitalopram (3–4% of control, not significant) or venlafaxine (7–8% of control, not significant). A significantly higher intensity of TUBB3 expression was observed after treatment with 5 μ M 5-HT (Fig. 8).

3.6. Antidepressants down-regulated neuronal outgrowth in differentiating SH-SY5Y neurons

The SH-SY5Y neurons were still growing and expanding the neurite network at the time of analysis, thus continuing the maturation processes, different from undifferentiated SH-SY5Y cells (Fig. 9). First, we assessed whether neuronal outgrowth is dependent on BDNF, utilizing 50 ng/mL recombinant BDNF and 3 μ g/mL anti-BDNF antibodies, as well as a TrkA receptor inhibitor (GW 441756) that was used as a negative control (Fig. 9, A). BDNF increased neurite outgrowth, whereas

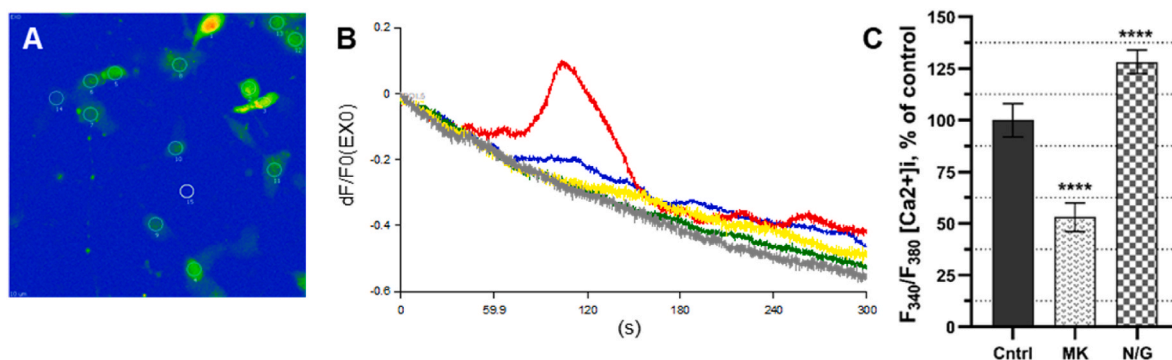


Fig. 4. Calcium in differentiating SH-SY5Y neurons on DIV21. A: Andor camera image shows SH-SY5Y neurons loaded with Cal-520 calcium dye. B: Spontaneous calcium signals in circled SH-SY5Y neurons (A) with Cal-520 fluorescent dye. C: Ca^{2+} -influx measurement with Fura-2, MK: NMDA receptor antagonist (MK-801) 10 μ M, and N/G: NMDA/glycine 100/50 μ M. Data are presented as normalized ratiometric values relative to the average of the control, and means are given with standard deviations. Each independent value is the mean of 4–8 technical replicates. Data were analyzed with a one-way ANOVA, with Dunnett's multiple comparisons test. **** $p < 0.0001$.

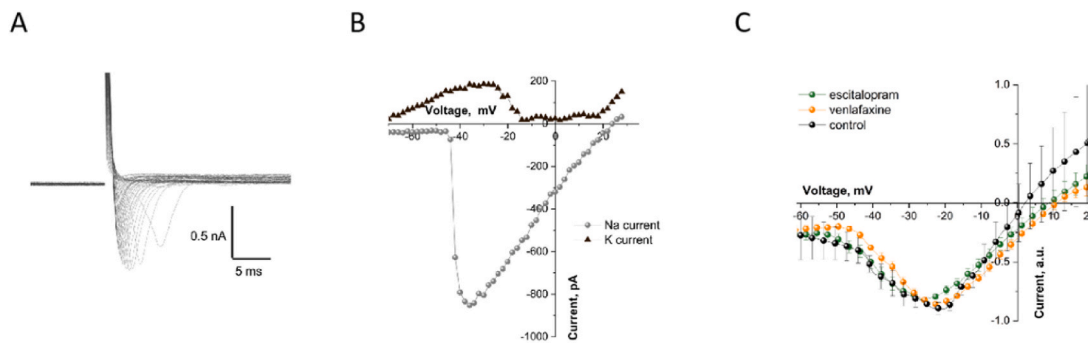


Fig. 5. Electrophysiological recordings from SH-SY5Y neurons. Original traces of whole-cell currents (A, traces of a representative cell from the escitalopram group) were recorded following 10 mV voltage steps in a range of -80 and $+40$ mV (B, its corresponding I/V curve) from each exposure group. The averaged I/V curve for each corresponding treatment group (C), where individual I/V curves were normalized to the maximum current amplitude.

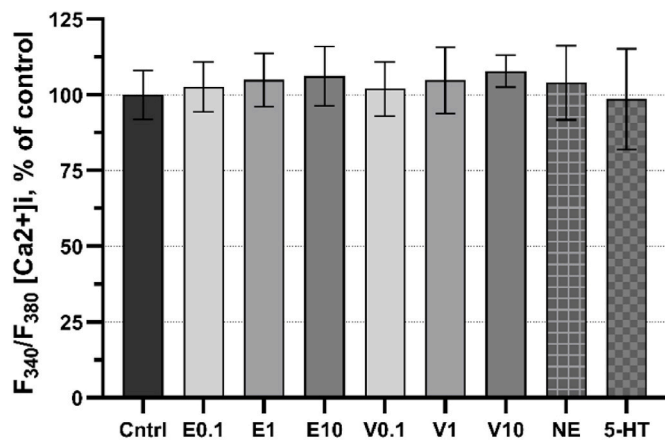


Fig. 6. The effects of antidepressants on calcium influx in differentiating SH-SY5Y neurons on DIV21. Neurons were exposed for 120 min to escitalopram oxalate (E) or venlafaxine hydrochloride (V) in concentrations of 0.1, 1, and 10 μ M; norepinephrine (NE) 1 μ M, or 5-hydroxytryptamine (5-HT) 5 μ M. Data were analyzed with a one-way ANOVA with Tukey's multiple comparisons test and presented as normalized values relative to the average of the control, and means are given with standard deviations.

neurons exposed to 5-HT did not show a significant increase. In contrast, exposure to anti-BDNF antibodies, and TrkA inhibitor GW 441756 reduced neurite length. Both ADDs negatively affected neurite outgrowth through 48 h (Fig. 9B and C), which was significant for 10 μ M concentrations of venlafaxine after 48 h. For escitalopram, 10 μ M, a tendency for a decrease was observed ($p = 0.206$).

4. Discussion

The present work was performed to improve our understanding of the complex interactions between the environment and the developing brain. Prenatal maternal depression has been linked to undesirable newborn outcomes, including lower gestational age and lower birth-weight (Field et al., 2008), neurobehavioral deviations in children (Smith et al., 2020), and also risks of maternal suicide if no active treatment is presented (Khalifeh et al., 2016). Unfortunately, ADD usage during pregnancy has also been associated with neurological and behavioral deviations in the offspring (Olivier et al., 2015; Brandlistuen et al., 2015; Chambers et al., 1996; Udechuku et al., 2010). Therefore, it is essential to investigate how these medications affect the developing human brain. ADDs are among the most commonly prescribed medications for patients with major depressive disorder. The positive effects of ADDs medication on the mood of patients are well-documented (Cipriani et al., 2018), but the exact mechanisms by which these

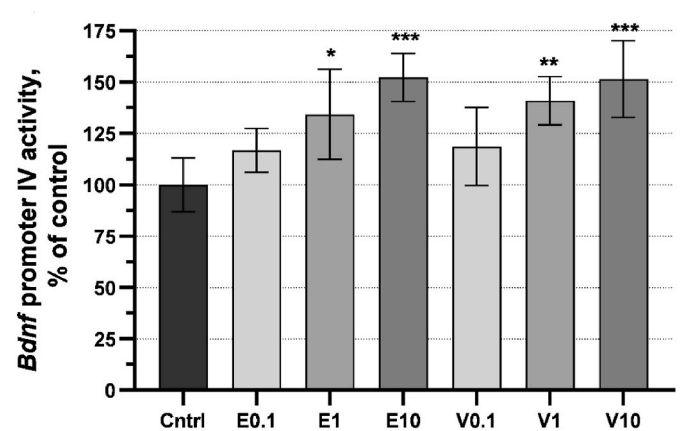


Fig. 7. The effects of antidepressants on activity-dependent *BDNF* promoter IV activation in differentiating SH-SY5Y neurons. The cells were exposed for 48 h to escitalopram oxalate (E) or venlafaxine hydrochloride (V) in concentrations of 0.1, 1, and 10 μ M. The *Firefly* luciferase activity of the *BDNF* pIV was measured 48 h after transfection using a standard luciferase assay. The level was adjusted to an internal *Renilla* transfection control. Data are presented as normalized values relative to the average of the control, and means are given with standard deviations. Each independent value is the mean of 4–6 technical replicates. Data were analyzed with a one-way ANOVA with Tukey's multiple comparisons test. * $p < 0.05$, ** $p < 0.01$, *** $p < 0.001$.

medications alter the brain are not entirely understood. Around 20% of pregnant women (Marcus et al., 2003) have symptoms of or suffer from depression, and the global burden seems to be growing, with now antenatal depression prevalence ranging from 15 to 65% (Dadi et al., 2020), while only 1 out of 7 of these patients received any formal treatment (Marcus et al., 2003).

Such neuromediators as 5-HT (Gaspar et al., 2003; Whitaker-Azmitia, 2001) and norepinephrine (also known as noradrenaline) (Saboori et al., 2020) function as neurotrophic factors during brain development, suggesting that changes in monoamine levels brought on by ADDs use may have an impact on neurodevelopment, including cell differentiation, proliferation, and migration. Either hyper- or hyposerotonemia may lead to neurobehavioral disorders, e.g., ASD (Rosenfeld, 2020; Shah et al., 2018). Thus, we hypothesized that escitalopram, as an SSRI and via increase of 5-HT, and venlafaxine, as an SNRI and via increase of 5-HT and norepinephrine, would have neurodevelopmental effects when presented to developing neurons. Escitalopram and venlafaxine serve as good representatives of their corresponding SSRI and SNRI subclasses of ADDs; both can be prescribed for patients during pregnancy and cross blood-brain/placental barriers (Schoretsanitis et al., 2021). The experimental concentrations of ADDs were chosen based on clinical information, where maternal and umbilical cord

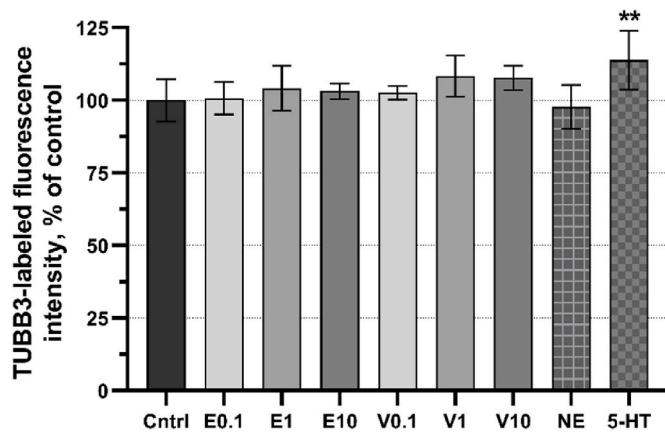


Fig. 8. The effects of antidepressants on TUBB3 neuronal marker in differentiating SH-SY5Y neurons. The cells were exposed for 48 h to escitalopram oxalate (E) or venlafaxine hydrochloride (V) in concentrations of 0.1, 1, and 10 μ M. Norepinephrine (NE) 1 μ M and serotonin (5-HT) 5 μ M were used as controls. The neurons were immunostained for TUBB3, and immunofluorescence was measured with a plate reader. Data are presented as normalized values relative to the average of the control, and means are given with standard deviations. Each independent value is the mean of 4–10 technical replicates. Data were analyzed with a one-way ANOVA with Tukey's multiple comparisons test. ** $p < 0.01$.

plasma concentrations for escitalopram were 0.011–0.23 μ M (4.5–94 ng/mL) and 0.011–0.13 μ M (4.4–54 ng/mL), while for a venlafaxine concentration range of maternal and umbilical cord plasma was 0.025–7.3 μ M (7.8–2283 ng/mL) and 0.004–5.4 μ M (1.4–1694 ng/mL), respectively (Schoetsanitis et al., 2021). In our experiments, we have used concentrations between 0.1 and 10 μ M, which includes clinical concentrations and above but not toxic.

The ability to access neuronal cell lines in the laboratory allows for the generation of models to study the impact of drugs on neuronal changes or the function of pathways. To study whether escitalopram or venlafaxine brings up developmental alterations in differentiating neurons, we utilized human neuroblastoma SH-SY5Y cells differentiated with RA as a model. SH-SY5Y cells are heterogeneous, consisting of neuroblast- and epithelial-like cells, which give characteristics of immature catecholaminergic neurons (Kovalevich and Langford, 2013). Depending on media conditions, SH-SY5Y cells can be differentiated toward various adult neuronal phenotypes, including cholinergic, adrenergic, or dopaminergic (Kovalevich and Langford, 2013; Kovalevich et al., 2021). Previously, shorter differentiation protocols have been used with RA-induction of differentiation or by co-induction with RA and BDNF (Goldie et al., 2014; Dravid et al., 2021). We approached SH-SY5Y neuronal differentiation with a lengthier protocol since cells started to show distinguishable neuron-like morphology in the culture after DIV14. By reseeding the cells after DIV17, we focused on neuronal-like differentiated cells in our model and aimed to see the neural regrowth of these neuronal-like differentiated cells with and without exposure to ADDs. For the undifferentiated control, we waited for the same number of days (DIV4) after seeding undifferentiated cells.

SH-SY5Y cells have been extensively used for the assessment of neuroactive pharmaceuticals and modeling of neurological disorders, e. g., Parkinson's (Xie et al., 2010) and Alzheimer's (Agholme et al., 2010), as well as depression, and ADDs studies (Correia et al., 2022; Guo et al., 2016; Cavarec et al., 2013; Wang et al., 2015), proving the potential to serve as an *in vitro* model to study the development of depression and its underlying neurobiological mechanisms. This study aimed to use SH-SY5Y cells as a model to study the effects of ADDs treatment on the differentiating neurons. This was achieved by assessing the neuronal differentiation of SH-SY5Y cells in the presence of RA and different ADD concentrations. We demonstrate that SH-SY5Y cells can be differentiated

toward a neuronal phenotype. Our findings suggest that differentiating SH-SY5Y neurons could provide a valuable model for further analysis of ADD effects on neurodevelopmental processes, as they express neuronal markers, BDNF, and undergo neurite elongation while not fully electrophysiologically mature.

In spite of the fact that SH-SY5Y cells and -derived neurons are an established model for neurobiology and neuropharmacology, to date, there are few electrophysiology studies made in SH-SY5Y (Şahin et al., 2021; Santillo et al., 2014; Cai et al., 2022). To the best of our knowledge, this is the first assessment of the electrophysiological profile of SH-SY5Y neurons under exposure to ADDs. Probably due to its cellular heterogeneity and/or neuronal immaturity, only a fraction of SH-SY5Y cells showed activated voltage-gated sodium channels during patch-clamp experiments. Those were tetrodotoxin-sensitive, and the latter is known to shape the action potential firing in neurons, thus confirming its neuronal origin. Notably, a higher percentage of cells exhibited Na^+ currents in cultures treated with ADDs, whereas in the venlafaxine group, more than half of all cells had prominent Na^+ currents. No change in electrophysiological properties of Na^+ and K^+ currents was seen with ADDs.

A new systematic review from 2022 on the serotonin theory claims no association between serotonin and depression (Moncrieff et al., 2022), which implies mechanisms other than SERT-dependent inhibition be involved in ADDs action. The BDNF hypothesis of depression has been widely discussed regarding depression and antidepressant efficacy (Groves, 2007; Björkholm and Monteggia, 2016; Yang et al., 2020). A recent study showed that ADDs could act by directly binding to TrkB neurotrophin receptors (Casarotto et al., 2021), thus activating BDNF signaling. Furthermore, BDNF self-amplifying autocrine loop (Acheson et al., 1995; Cheng et al., 2011) suggests potentiating and prolonged effects. In our experiments, SH-SY5Y neurons responded to ADD treatments in a concentration-dependent manner, where activity-dependent BDNF promoter IV (−204/+320) activation was gradually up-regulated with higher concentrations of escitalopram or venlafaxine. The BDNF promoter IV (formerly known as promoter III) is the one that responds most strongly to neural activity (Hong et al., 2008; Park and Poo, 2013). In fact, different patterns of stimuli represented by Ca^{2+} and/or cAMP signals control BDNF promoter IV (He et al., 2005; Tao et al., 2002; Sakata et al., 2009). Even though cytosolic calcium measurements did not show any significant effect after 120-min ADD exposure in our experiments, a slightly positive trend toward an increase could be observed.

BDNF is expressed in the developing and adult brain, affecting neurons positively or negatively through various intracellular signaling via activation of its TrkB- or p75 neurotrophin receptor (p75NTR) receptors (Numakawa et al., 2010), depending on cellular and molecular contexts. Mature BDNF mainly acts through the TrkB receptor, while pro-BDNF – preferentially via p75NTR, and those underlying signaling pathways potentiate opposite effects (Castrén and Kojima, 2017; Duman et al., 2021). Regulated and activity-dependent BDNF release activates BDNF/TrkB signaling and leads to (among others) cellular differentiation, arborization, and survival; whereas pro-BDNF is constitutively released, and activates the pro-BDNF/p75NTR cascade, leading to pruning, decreased growth and apoptosis. Our data suggest that neurite outgrowth down-regulation under treatment with ADDs in differentiating SH-SY5Y neurons is likely due to pro-BDNF/BDNF presence and activation of p75NTR downstream pathways. Although, we cannot exclude neurotrophins other than pro-BDNF/BDNF that have an affinity to p75NTR (NGF, NT-3, NT-4 and their respective pro-forms) (Bibel et al., 1999; Malik et al., 2021) and the balancing effects of other guiding factors involved in neurite outgrowth, which can also indicate BDNF-independent neurite suppression. In fact, SH-SY5Y neurite outgrowth was markedly reduced by TrkA receptor inhibition, implying more complex regulatory machinery involved.

The 5-HT and BDNF interactions play an important role in essential developmental processes in the developing and adult brain (Popova and

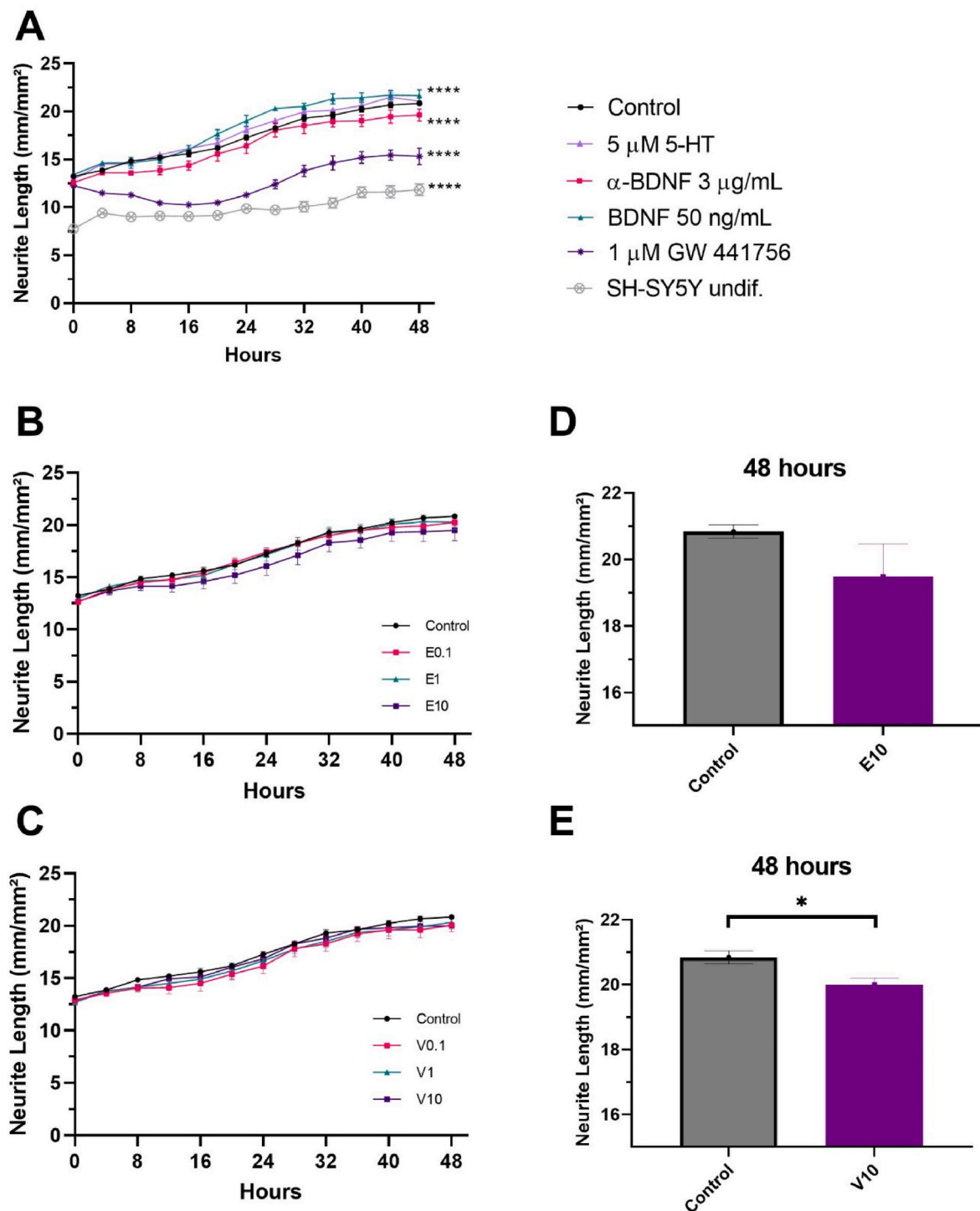


Fig. 9. Neurite outgrowth in differentiating SH-SY5Y neurons. The cells were exposed for 48 h to recombinant BDNF, anti-BDNF antibodies or TrkA inhibitor (5 μ M) GW 441756 (A); and escitalopram oxalate (E) or venlafaxine hydrochloride (V) in concentrations of 0.1, 1 and 10 μ M (B, C). Data are presented as normalized values relative to the average of the control, and means are given with standard deviations. Each independent value is the mean of 3–6 technical replicates. Data were analyzed with two-way ANOVA. ** $p < 0.01$, **** $p < 0.0001$. Neurite lengths for escitalopram oxalate (D) or venlafaxine hydrochloride (E) at 48 h. Data were analyzed for the 48-h time point, each drug is compared to control and analyzed with Student's *t*-test * $p < 0.05$.

Naumenko, 2019; Martinowich and Lu, 2008; Homberg et al., 2014). They share common downstream effectors, can modulate one another, and have been proposed as mechanistic explanations for the development of neuropsychiatric disorders (Popova and Naumenko, 2019; Martinowich and Lu, 2008; Homberg et al., 2014). 5-HT induced BDNF expression and up-regulated BDNF protein level in rat raphe nuclei neuronal cultures at embryonic day 14 (Galter and Unsicker, 2000).

Although the pro-BDNF/p75NTR primarily manifests pro-apoptotic effects (Ichim et al., 2012), this pathway shares common underlying effectors with 5-HT receptors that affect non-apoptotic functions (Popova and Naumenko, 2019; Kraemer et al., 2014).

In differentiating rat neural stem cells, BDNF treatment did not change the expression of the TUBB3 protein (Langhnoja et al., 2021). On the other hand, BDNF increased the percentage of differentiated cells

expressing TUBB3 in mouse retinal neurospheres (De Melo Reis et al., 2011). TUBB3 is associated with neuronal growth and migration (Poirier et al., 2010; Saillour et al., 2014). It has been shown that ADDs, particularly escitalopram, disrupt α -tubulin complexes (Singh et al., 2018). In addition, TUBB3 was shown to be down-regulated by venlafaxine after 1 day of neuronally differentiating NCCIT cells (Doh et al., 2015). Since the data on TUBB3 and ADD interactions vary, we assessed TUBB3 in our experiments. We observed a tendency to increase TUBB3 expression in differentiating SH-SY5Y neurons. Although there was a trend toward TUBB3 up-regulation under treatment with ADDs, neurite measurements revealed a negative effect of ADDs on neurite outgrowth in differentiating SH-SY5Y neurons through 48-h exposure.

Studies focusing on ADDs show neurite increase in rat PC12 cells (Meng et al., 2019; Gao et al., 2020), and some studies demonstrate neuroprotective effects upon addition of ADDs (Morello et al., 2021; Jantas et al., 2008). There is also evidence in the literature on axonal regeneration in adult rodents upon exposure of ADDs (Nakamura, 1990, 1991). In contrast, our model showed decreased neurite length in human SH-SY5Y cells. This could be due to the species difference, or that it represents a different developmental stage due to a narrow developmental window or cellular phenotype such as its neuroblastoma origin. Taken together, it is crucial to study different cell types at different developmental stages to have a better understanding of the effects of ADDs.

Changes identified in our study may represent links to molecular processes of importance to depression, as well as to be involved in neurodevelopmental alterations observed in postpartum children that were exposed to ADDs antenatally, such as ASD (Rai et al., 2013; Fatima et al., 2018), ADHD (Leshem et al., 2021), anxiety (Brandlistuen et al., 2015), and abnormal psychomotor development (Mortensen et al., 2003). Future research should elucidate the roles of the identified alterations in the developing brain, mechanistic studies, and the relevance of the observed changes to findings in offspring exposed to ADDs prenatally. The effects of these ADDs on the developing fetus should be investigated further in *in vivo* models, as well as the mechanisms of action by which these medications act on the human brain. It is crucial to provide accurate information to the public regarding the risks and benefits of medication use during pregnancy and improve the current paradigm of care for antenatal depression.

5. Conclusion

This work establishes differentiating SH-SY5Y neurons as a neurodevelopmental model to identify ADD-induced neuronal changes for the first time in the literature. Our results demonstrate that ADDs up-regulate the activity-dependent *BDNF* promoter in differentiating neurons but down-regulate neurite outgrowth, the latter contrasting to adult neurons.

Author statement

Please find enclosed a manuscript entitled “Antidepressants escitalopram and venlafaxine up-regulate *BDNF* promoter IV but down-regulate neurite outgrowth in differentiating SH-SY5Y neurons” authored by Denis Zosen, Elena Kondratskaya, Oyukum Kaplan-Arabaci, Fred Haugen, and Ragnhild Elisabeth Paulsen to be considered for publication as a full length article in “Neurochemistry International”.

The authorship is based on ICJME recommendations. Both the authors and the institution where the work has been carried out have approved the submission for publication. Authors declare no conflict of interest. We understand that if the manuscript is accepted for publication, copyright in the article shall be assigned exclusively to the Publisher.

Ethical procedure

- The research meets all applicable standards with regard to the ethics of experimentation and research integrity, and the following is being certified/declared true and stated within the article.

- As an expert scientist and along with co-authors of the concerned field, this paper has been submitted with full responsibility, following due ethical procedure, and there is no duplicate publication, fraud, plagiarism, or concerns about animal or human experimentation.

A disclosure/conflict of interest statement:

- None of the authors of this paper has a financial or personal relationship with other people or organizations that could inappropriately influence or bias the content of the paper.

- It is to specifically state that “No Competing interests are at stake and there is No Conflict of Interest” with other people or organizations that could inappropriately influence or bias the content of the paper.

Declaration of competing interest

The authors declare that they have no known competing financial interests or personal relationships that could have appeared to influence the work reported in this paper.

Data availability

Data will be made available on request.

Acknowledgments

The authors want to thank Prof. Joel C. Glover and Prof. Srdjan Djurovic for providing access to the electrophysiology and calcium imaging equipment at the Department of Medicine, University of Oslo; and Beata Urbanczyk Mohebi (Department of Pharmacy, University of Oslo), Dr. Oddvar Myhre, Dr. Igor Snapkow, and Dina Behmen for the technical assistance with high content analysis at the Norwegian Institute of Public Health. This work was supported by the Nansen Foundation.

Appendix A. Supplementary data

Supplementary data to this article can be found online at <https://doi.org/10.1016/j.neuint.2023.105571>.

References

- Acheson, A., Conover, J.C., Fandl, J.P., DeChiara, T.M., Russell, M., Thadani, A., et al., 1995. A *BDNF* autocrine loop in adult sensory neurons prevents cell death. *Nature* 374 (6521), 450–453.
- Agholme, L., Lindström, T., Kägedal, K., Marcusson, J., Hallbeck, M., 2010. An *in vitro* model for neuroscience: differentiation of SH-SY5Y cells into cells with morphological and biochemical characteristics of mature neurons. *J. Alzheim. Dis.* 20 (4), 1069–1082.
- Albert, P.R., Benkelfat, C., Descarries, L., 2012. The Neurobiology of Depression—Revisiting the Serotonin Hypothesis. I. Cellular and Molecular Mechanisms. *The Royal Society*, pp. 2378–2381.
- Alwan, S., Reefhuis, J., Rasmussen, S.A., Friedman, J.M., Nbdp, Study, 2011. Patterns of antidepressant medication use among pregnant women in a United States population. *J. Clin. Pharmacol.* 51 (2), 264–270.
- Bibel, M., Hoppe, E., Barde, Y.-A., 1999. Biochemical and functional interactions between the neurotrophin receptors *trk* and *p75NTR*. *EMBO J.* 18 (3), 616–622.
- Björkholm, C., Monteggia, L.M., 2016. *BDNF*—a key transducer of antidepressant effects. *Neuropharmacology* 102, 72–79.
- Brandlistuen, R.E., Ystrom, E., Eberhard-Gran, M., Nulman, I., Koren, G., Nordeng, H., 2015. Behavioural effects of fetal antidepressant exposure in a Norwegian cohort of discordant siblings. *Int. J. Epidemiol.* 44 (4), 1397–1407.
- Cai, A., Lin, Z., Liu, N., Li, X., Wang, J., Wu, Y., et al., 2022. Neuroblastoma SH-SY5Y cell differentiation to mature neuron by AM580 treatment. *Neurochem. Res.* 47 (12), 3723–3732.
- Casarotto, P.C., Gyrych, M., Fred, S.M., Kovaleva, V., Moliner, R., Enkavi, G., et al., 2021. Antidepressant drugs act by directly binding to TRKB neurotrophin receptors. *Cell* 184 (5), 1299–313. e19.
- Castrén, E., Kojima, M., 2017. Brain-derived neurotrophic factor in mood disorders and antidepressant treatments. *Neurobiol. Dis.* 97, 119–126.

- Castre n, E., Monteggia, L.M., 2021. Brain-derived neurotrophic factor signaling in depression and antidepressant action. *Biol. Psychiatr.* 90 (2), 128–136.
- Cavarec, L., Vincent, L., Le Borgne, C., Plusquellec, C., Ollivier, N., Normandie-Levi, P., et al., 2013. In vitro screening for drug-induced depression and/or suicidal adverse effects: a new toxicogenomic assay based on CE-SSCP analysis of HTR2C mRNA editing in SH-SY5Y cells. *Neurotox. Res.* 23 (1), 49–62.
- Chambers, C.D., Johnson, K.A., Dick, L.M., Felix, R.J., Jones, K.L., 1996. Birth outcomes in pregnant women taking fluoxetine. *N. Engl. J. Med.* 335 (14), 1010–1015.
- Cheng, P.-L., Song, A.-H., Wong, Y.-H., Wang, S., Zhang, X., Poo, M.-M., 2011. Self-amplifying autocrine actions of BDNF in axon development. *Proc. Natl. Acad. Sci. USA* 108 (45), 18430–18435.
- Cipriani, A., Furukawa, T.A., Salanti, G., Chaimani, A., Atkinson, L.Z., Ogawa, Y., et al., 2018. Comparative efficacy and acceptability of 21 antidepressant drugs for the acute treatment of adults with major depressive disorder: a systematic review and network meta-analysis. *Focus* 16 (4), 420–429.
- Coppen, A., 1967. The biochemistry of affective disorders. *Br. J. Psychiatr.* 113 (504), 1237–1264.
- Correia, A.S., Fraga, S., Teixeira, J.P., Vale, N., 2022. Cell model of depression: reduction of cell stress with mirtazapine. *Int. J. Mol. Sci.* 23 (9), 4942.
- Dadi, A.F., Miller, E.R., Bisetegn, T.A., Mwanri, L., 2020. Global burden of antenatal depression and its association with adverse birth outcomes: an umbrella review. *BMC Publ. Health* 20 (1), 1–16.
- De Melo Reis, R., Schitine, C., Kofalvi, A., Grade, S., Cortes, L., Gardino, P., et al., 2011. Functional identification of cell phenotypes differentiating from mice retinal neurospheres using single cell calcium imaging. *Cell. Mol. Neurobiol.* 31 (6), 835–846.
- Doh, M.S., Oh, D.H., Kim, S.H., Choi, M.R., Chai, Y.G., 2015. Profiling of proteins regulated by venlafaxine during neural differentiation of human cells. *Psychiatry Investigation* 12 (1), 81.
- Dravid, A., Raos, B., Svirskis, D., O’Carroll, S.J., 2021. Optimised techniques for high-throughput screening of differentiated SH-SY5Y cells and application for neurite outgrowth assays. *Sci. Rep.* 11 (1), 1–15.
- Dubovicky, M., Belovicova, K., Csatlosova, K., Bogi, E., 2017. Risks of using SSRI/SNRI antidepressants during pregnancy and lactation. *Interdiscipl. Toxicol.* 10 (1), 30.
- Duman, R.S., Deyama, S., Foga a, M.V., 2021. Role of BDNF in the pathophysiology and treatment of depression: activity-dependent effects distinguish rapid-acting antidepressants. *Eur. J. Neurosci.* 53 (1), 126–139.
- Fatima, Z., Zahra, A., Ghouse, M., Wang, X., Yuan, Z., 2018. Maternal SSRIs experience and risk of ASD in offspring: a review. *Toxicology research* 7 (6), 1020–1028.
- Field, T., Diego, M., Hernandez-Reif, M., Figueiredo, B., Schanberg, S., Kuhn, C., et al., 2008. Chronic prenatal depression and neonatal outcome. *Int. J. Neurosci.* 118 (1), 95–103.
- Galter, D., Unsicker, K., 2000. Brain-derived neurotrophic factor and trkB are essential for cAMP-mediated induction of the serotonergic neuronal phenotype. *J. Neurosci. Res.* 61 (3), 295–301.
- Gao, W., Chen, R., Xie, N., Tang, D., Zhou, B., Wang, D., 2020. Duloxetine-induced neural cell death and promoted neurite outgrowth in N2a cells. *Neurotox. Res.* 38 (4), 859–870.
- Gaspar, P., Cases, O., Maroteaux, L., 2003. The developmental role of serotonin: news from mouse molecular genetics. *Nat. Rev. Neurosci.* 4 (12), 1002–1012.
- Gentile, S., Fusco, M.L., 2017. Placental and fetal effects of antenatal exposure to antidepressants or untreated maternal depression. *J. Matern. Fetal Neonatal Med.* 30 (10), 1189–1199.
- Goldie, B.J., Barnett, M.M., Cairns, M.J., 2014. BDNF and the maturation of posttranscriptional regulatory networks in human SH-SY5Y neuroblast differentiation. *Front. Cell. Neurosci.* 8, 325.
- Groves, J., 2007. Is it time to reassess the BDNF hypothesis of depression? *Mol. Psychiatr.* 12 (12), 1079–1088.
- Guo, J., Zhang, W., Zhang, L., Ding, H., Zhang, J., Song, C., et al., 2016. Probable involvement of p11 with interferon alpha induced depression. *Sci. Rep.* 6 (1), 1–15.
- He, J., Gong, H., Luo, Q., 2005. BDNF acutely modulates synaptic transmission and calcium signalling in developing cortical neurons. *Cell. Physiol. Biochem.* 16 (1–3), 69–76.
- Herlenius, E., Lagercrantz, H., 2001. Neurotransmitters and neuromodulators during early human development. *Early Hum. Dev.* 65 (1), 21–37.
- Homberg, J.R., Molteni, R., Calabrese, F., Riva, M.A., 2014. The serotonin–BDNF duo: developmental implications for the vulnerability to psychopathology. *Neurosci. Biobehav. Rev.* 43, 35–47.
- Hong, E.J., McCord, A.E., Greenberg, M.E., 2008. A biological function for the neuronal activity-dependent component of Bdnf transcription in the development of cortical inhibition. *Neuron* 60 (4), 610–624.
- Ichim, G., Tauszig-Delamasure, S., Mehlen, P., 2012. Neurotrophins and cell death. *Exp. Cell Res.* 318 (11), 1221–1228.
- Jantas, D., Pytel, M., Mozrzyms, J.W., Leskiewicz, M., Regulska, M., Antkiewicz-Michaluk, L., et al., 2008. The attenuating effect of memantine on staurosporine-, salsolinol- and doxorubicin-induced apoptosis in human neuroblastoma SH-SY5Y cells. *Neurochem. Int.* 52 (4–5), 864–877.
- Katsetos, C.D., Legido, A., Perentes, E., M rk, S.J., 2003. Class III β -tubulin isotype: a key cytoskeletal protein at the crossroads of developmental neurobiology and tumor neuropathology. *J. Child Neurol.* 18 (12), 851–866.
- Kautzky, A., Slamanig, R., Unger, A., H flich, A., 2022. Neonatal outcome and adaption after in utero exposure to antidepressants: a systematic review and meta-analysis. *Acta Psychiatr. Scand.* 145 (1), 6–28.
- Khalifeh, H., Hunt, I.M., Appleby, L., Howard, L.M., 2016. Suicide in perinatal and non-perinatal women in contact with psychiatric services: 15 year findings from a UK national inquiry. *Lancet Psychiatr.* 3 (3), 233–242.
- Kovalevich, J., Langford, D., 2013. Neuronal cell culture: springer. In: Considerations for the Use of SH-SY5Y Neuroblastoma Cells in Neurobiology, pp. 9–21.
- Kovalevich, J., Santerre, M., Langford, D., 2021. Neuronal cell culture: springer. In: Considerations for the Use of SH-SY5Y Neuroblastoma Cells in Neurobiology, pp. 9–23.
- Kraemer, B., Yoon, S.O., Carter, B., 2014. The biological functions and signaling mechanisms of the p75 neurotrophin receptor. In: *Neurotrophic Factors*, pp. 121–164. Springer.
- Langhnoja, J., Buch, L., Pillai, P., 2021. Potential role of NGF, BDNF, and their receptors in oligodendrocytes differentiation from neural stem cell: an in vitro study. *Cell Biol. Int.* 45 (2), 432–446.
- Lauv s, A.J., Lislien, M., Holme, J.A., Dirven, H., Paulsen, R.E., Alm, I.M., et al., 2022. Developmental neurotoxicity of acrylamide and its metabolite glycidamide in a human mixed culture of neurons and astrocytes undergoing differentiation in concentrations relevant for human exposure. *Neurotoxicology* 92, 33–48.
- Lee, B.-H., Kim, Y.-K., 2010. The roles of BDNF in the pathophysiology of major depression and in antidepressant treatment. *Psychiatry investigation* 7 (4), 231.
- Leshem, R., Bar-Oz, B., Diav-Citrin, O., Gbaly, S., Soliman, J., Renoux, C., et al., 2021. Selective serotonin reuptake inhibitors (SSRIs) and serotonin norepinephrine reuptake inhibitors (SNRIs) during pregnancy and the risk for autism spectrum disorder (ASD) and attention deficit hyperactivity disorder (ADHD) in the offspring: a true effect or a bias? A systematic review & meta-analysis. *Curr. Neuropharmacol.* 19 (6), 896–906.
- Malik, S.C., Sozmen, E.G., Baeza-Raja, B., Le Moan, N., Akassoglou, K., Schachtrup, C., 2021. In vivo functions of p75NTR: challenges and opportunities for an emerging therapeutic target. *Trends Pharmacol. Sci.* 42 (9), 772–788.
- Marcus, S.M., Flynn, H.A., Blow, F.C., Barry, K.L., 2003. Depressive symptoms among pregnant women screened in obstetrics settings. *J. Wom. Health* 12 (4), 373–380.
- Martinowich, K., Lu, B., 2008. Interaction between BDNF and serotonin: role in mood disorders. *Neuropsychopharmacology* 33 (1), 73–83.
- Meng, P., Zhu, Q., Yang, H., Liu, D., Lin, X., Liu, J., et al., 2019. Leonurine promotes neurite outgrowth and neurotrophic activity by modulating the GR/SGK1 signaling pathway in cultured PC12 cells. *Neuroreport* 30 (4), 247–254.
- Moncrieff, J., Cooper, R.E., Stockmann, T., Amendola, S., Hengartner, M.P., Horowitz, M.A., 2022. The serotonin theory of depression: a systematic umbrella review of the evidence. *Mol. Psychiatr.* 1–14.
- Morello, G., Villari, A., Spampinato, A.G., La Cognata, V., Guarnaccia, M., Gentile, G., et al., 2021. Transcriptional profiles of cell fate transitions reveal early drivers of neuronal apoptosis and survival. *Cells* 10 (11).
- Mortensen, J., Olsen, J., Larsen, H., Bendsen, J., Obel, C., S rensen, H., 2003. Psychomotor development in children exposed in utero to benzodiazepines, antidepressants, neuroleptics, and anti-epileptics. *Eur. J. Epidemiol.* 18 (8), 769–771.
- Nakamura, S., 1990. Antidepressants induce regeneration of catecholaminergic axon terminals in the rat cerebral cortex. *Neurosci. Lett.* 111 (1–2), 64–68.
- Nakamura, S., 1991. Axonal sprouting of noradrenergic locus coeruleus neurons following repeated stress and antidepressant treatment. *Prog. Brain Res.* 88, 587–598.
- Nulman, I., Rovet, J., Stewart, D.E., Wolpin, J., Gardner, H.A., Theis, J.G., et al., 1997. Neurodevelopment of children exposed in utero to antidepressant drugs. *N. Engl. J. Med.* 336 (4), 258–262.
- Numakawa, T., Suzuki, S., Kumamaru, E., Adachi, N., Richards, M., Kunugi, H., 2010. BDNF function and intracellular signaling in neurons. *Histol. Histopathol.* 25 (2), 237–258.
- Olivier, J.D.,  kerud, H., Poromaa, I.S., 2015. Antenatal depression and antidepressants during pregnancy: unraveling the complex interactions for the offspring. *Eur. J. Pharmacol.* 753, 257–262.
- Park, H., Poo, M.-m., 2013. Neurotrophin regulation of neural circuit development and function. *Nat. Rev. Neurosci.* 14 (1), 7–23.
- Poirier, K., Saillour, Y., Bahi-Buisson, N., Jaglin, X.H., Fallet-Bianco, C., Nabbout, R., et al., 2010. Mutations in the neuronal α -tubulin subunit TUBB3 result in malformation of cortical development and neuronal migration defects. *Hum. Mol. Genet.* 19 (22), 4462–4473.
- Popova, N.K., Naumenko, V.S., 2019. Neuronal and behavioral plasticity: the role of serotonin and BDNF systems tandem. *Expert Opin. Ther. Targets* 23 (3), 227–239.
- Pruunsild, P., Sepp, M., Orav, E., Koppel, I., Timmus, T., 2011. Identification of cis-elements and transcription factors regulating neuronal activity-dependent transcription of human BDNF gene. *J. Neurosci.* 31 (9), 3295–3308.
- Rai, D., Lee, B.K., Dalman, C., Golding, J., Lewis, G., Magnusson, C., 2013. Parental depression, maternal antidepressant use during pregnancy, and risk of autism spectrum disorders: population based case-control study. *Br. Med. J.* 346.
- Rosenfeld, C.S., 2020. Placental serotonin signaling, pregnancy outcomes, and regulation of fetal brain development. *Biol. Reprod.* 102 (3), 532–538.
- Saboory, E., Ghasemi, M., Mehranfar, N., 2020. Norepinephrine, neurodevelopment and behavior. *Neurochem. Int.* 135, 104706.
-  ahin, M.,  nc , G., Yilmaz, M.A.,  zkan, D., Sayba lı, H., 2021. Transformation of SH-SY5Y cell line into neuron-like cells: investigation of electrophysiological and biomechanical changes. *Neurosci. Lett.* 745, 135628.
- Saillour, Y., Broix, L., Bruel-Jungerman, E., Lebrun, N., Muraca, G., Rucci, J., et al., 2014. Beta tubulin isoforms are not interchangeable for rescuing impaired radial migration due to Tubb3 knockdown. *Hum. Mol. Genet.* 23 (6), 1516–1526.
- Sakata, K., Woo, N.H., Martinowich, K., Greene, J.S., Schloesser, R.J., Shen, L., et al., 2009. Critical role of promoter IV-driven BDNF transcription in GABAergic transmission and synaptic plasticity in the prefrontal cortex. *Proc. Natl. Acad. Sci. USA* 106 (14), 5942–5947.

- Santillo, S., Moriello, A.S., Di Maio, V., 2014. Electrophysiological variability in the SH-SY5Y cellular line. *Gen. Physiol. Biophys.* 33 (1), 121–129.
- Schildkraut, J.J., 1965. The catecholamine hypothesis of affective disorders: a review of supporting evidence. *Am. J. Psychiatr.* 122 (5), 509–522.
- Schoretsanitis, G., Westin, A.A., Stingl, J.C., Deligiannidis, K.M., Paulzen, M., Spigset, O., 2021. Antidepressant transfer into amniotic fluid, umbilical cord blood & breast milk: a systematic review & combined analysis. *Prog. Neuro Psychopharmacol. Biol. Psychiatr.* 107, 110228.
- Shah, R., Courtiol, E., Castellanos, F.X., Teixeira, C.M., 2018. Abnormal serotonin levels during perinatal development lead to behavioral deficits in adulthood. *Front. Behav. Neurosci.* 12, 114.
- Singh, H., Wray, N., Schappi, J.M., Rasenick, M.M., 2018. Disruption of lipid-raft localized G α s/tubulin complexes by antidepressants: a unique feature of HDAC6 inhibitors, SSRI and tricyclic compounds. *Neuropsychopharmacology* 43 (7), 1481–1491.
- Smith, A., Twynstra, J., Seabrook, J.A., 2020. Antenatal depression and offspring health outcomes. *Obstet. Med.* 13 (2), 55–61.
- Strøm, B.O., Aden, P., Mathisen, G.H., Lømo, J., Davanger, S., Paulsen, R.E., 2010. Transfection of chicken cerebellar granule neurons used to study glucocorticoid receptor regulation by nuclear receptor 4A (NR4A). *J. Neurosci. Methods* 193 (1), 39–46.
- Szegda, K., Markenson, G., Bertone-Johnson, E.R., Chasan-Taber, L., 2014. Depression during pregnancy: a risk factor for adverse neonatal outcomes? A critical review of the literature. *J. Matern. Fetal Neonatal Med.* 27 (9), 960–967.
- Tao, X., West, A.E., Chen, W.G., Corfas, G., Greenberg, M.E., 2002. A calcium-responsive transcription factor, CaRF, that regulates neuronal activity-dependent expression of BDNF. *Neuron* 33 (3), 383–395.
- Then, C.-K., Liu, K.-H., Liao, M.-H., Chung, K.-H., Wang, J.-Y., Shen, S.-C., 2017. Antidepressants, sertraline and paroxetine, increase calcium influx and induce mitochondrial damage-mediated apoptosis of astrocytes. *Oncotarget* 8 (70), 115490.
- Thompson, B.L., Levitt, P., Stanwood, G.D., 2009. Prenatal exposure to drugs: effects on brain development and implications for policy and education. *Nat. Rev. Neurosci.* 10 (4), 303–312.
- Toselli, M., Tosetti, P., Taglietti, V., 1996. Functional changes in sodium conductances in the human neuroblastoma cell line SH-SY5Y during in vitro differentiation. *J. Neurophysiol.* 76 (6), 3920–3927.
- Tosetti, P., Taglietti, V., Toselli, M., 1998. Functional changes in potassium conductances of the human neuroblastoma cell line SH-SY5Y during in vitro differentiation. *J. Neurophysiol.* 79 (2), 648–658.
- Udechuku, A., Nguyen, T., Hill, R., Szego, K., 2010. Antidepressants in pregnancy: a systematic review. *Aust. N. Z. J. Psychiatr.* 44 (11), 978–996.
- Vetter, I., Mozar, C.A., Durek, T., Wingerd, J.S., Alewood, P.F., Christie, M.J., et al., 2012. Characterisation of Na(v) types endogenously expressed in human SH-SY5Y neuroblastoma cells. *Biochem. Pharmacol.* 83 (11), 1562–1571.
- Vigod, S.N., Wilson, C.A., Howard, L.M., 2016. Depression in pregnancy. *Br. Med. J.* 352.
- Wang, Y., Hilton, B.A., Cui, K., Zhu, M.-Y., 2015. Effects of antidepressants on DSP4/CPT-induced DNA damage response in neuroblastoma SH-SY5Y cells. *Neurotox. Res.* 28 (2), 154–170.
- Whitaker-Azmitia, P.M., 2001. Serotonin and brain development: role in human developmental diseases. *Brain Res. Bull.* 56 (5), 479–485.
- Xie, H-r, Hu, L-s, Li, G-y, 2010. SH-SY5Y human neuroblastoma cell line: in vitro cell model of dopaminergic neurons in Parkinson's disease. *Chin. Med. J.* 123 (8), 1086–1092.
- Yang, T., Nie, Z., Shu, H., Kuang, Y., Chen, X., Cheng, J., et al., 2020. The role of BDNF on neural plasticity in depression. *Front. Cell. Neurosci.* 14, 82.